Progress In Electromagnetics Research C, Vol. 70, 183–191, 2016

A Multiband and Omnidirectional, CPW-Fed Single-Layer Based Dual Tapered-Slot Antenna

Omar A. Saraereh*

Abstract—Travelling wave antennas such as Vivaldi antenna have conventionally been used for obtaining wideband and directional radiation pattern. This paper presents a novel way to obtain first of its kind, omnidirectional travelling wave antenna inspired by Vivaldi. Traditional omnidirectional antennas such as monopole and dipole rely on resonance condition which is usually satisfied on narrow band while the proposed antenna is relatively broadband owing to its travelling wave phenomenon. Moreover, typical Vivaldi antennas are double layered while our design requires only one layer. Antenna has been simulated and optimized in HFSS to operate in dual bands of UWB spectrum. The antenna has been measured and characterized using Keysight handheld VNA and Satimo Anechoic chamber. Good agreement between simulations and measurements has been obtained despite the fabrication tolerance of LPKF PCB manufacturing machine.

1. INTRODUCTION

Directional antennas find their typical applications in point to point communication, satellite communication and high resolution scanning. These types of antennas can be made using travelling wave (e.g., Vivaldi and slotted waveguide antennas) or resonance phenomenon (e.g., patch antenna). On the other hand, omnidirectional antennas are used for indoor communication and better range coverage. These types of antennas are typically based upon resonance phenomenon (e.g., dipole and monopole antennas) which is achievable usually in narrow band. Various techniques such as putting slots, parasitic element loading and defected ground plane are usually applied to make such antennas broadband [1]. To the best of the author's knowledge, this paper explains the design of the first CPW (Co-planar waveguide) fed, single-layer, dual tapered slots based broadband omnidirectional antenna with desirable down tilt for better coverage in a hemisphere.

Typical broadband and end-fire Vivaldi antennas have two types, the one with microstrip to slot transition [2–4] and the other with antipodal structure [5]. Typically, these antennas make use of both sides of the PCB [2, 5–7]. Some efforts have been made to design CPW-fed, single layer based Vivaldi antennas as the one shown in [8]. Overall size of the system can be reduced by using one side of PCB for designing the RF circuitry when dealing with single layer based antennas. The proposed antenna in this paper also makes use of a single layer only. The design of the proposed antenna is shown in the next section while its simulated and measured results are shown in the following sections. Conclusion is provided in Section 4.

2. ANTENNA DESIGN

Antenna is designed to be fed by CPW in order to keep the feed and radiating structure on a single layer of PCB as shown in Figure 1. As the design is inspired from a typical tapered slot (vivaldi) antenna, CPW to dual tapered slot transition is used as the two radiating elements to achieve omnidirectional radiation. Elliptically tapered profile ensures smooth field transition in the radiating element.

Received 22 November 2016, Accepted 24 December 2016, Scheduled 10 January 2017
* Corresponding author: Omar A. Saraereh (eloas2@hu.edu.jo).
The author is with the Electrical Engineering Department, Engineering Faculty, The Hashemite University, Zarqa 13115, Jordan.

Unlike a dipole antenna, radiating arms of the proposed antenna are not exactly 180° apart, rather they have mutual angle greater than 120°. Owing to the travelling wave nature of the design, the radiating donut can acquire desirable down-tilt. Radiation down-tilt and its advantages will be explained in detail in the section of results.

Figure 2 shows the annotated diagram of the antenna, designed in HFSS. The radiating slot size (L-slot) was initially designed for 3.1 GHz ($\lambda g/2 = 32$ mm). Though the slot size determines the lowest operating frequency of the antenna, its size is also directly proportional to its impedance. CPW is matched to 50 Ω while the slot offers high impedance. A smooth transition from CPW to elliptically tapered dual slots was needed to be optimized in HFSS using parametric analysis on the minor and

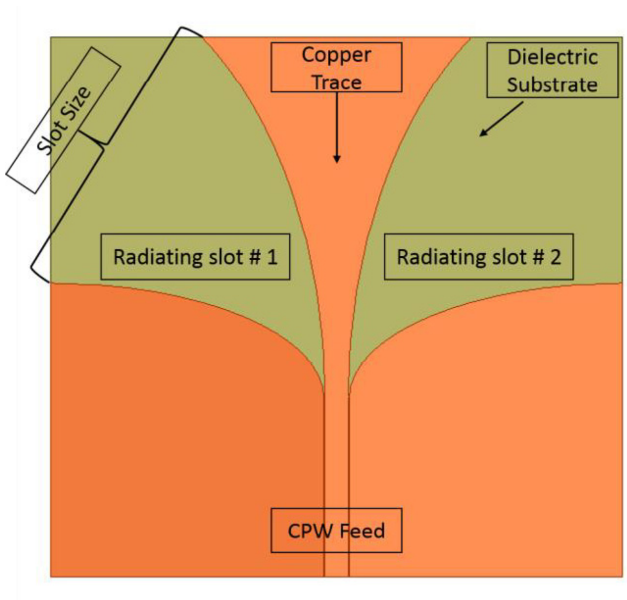

Figure 1. CPW to dual slot transition based antenna.

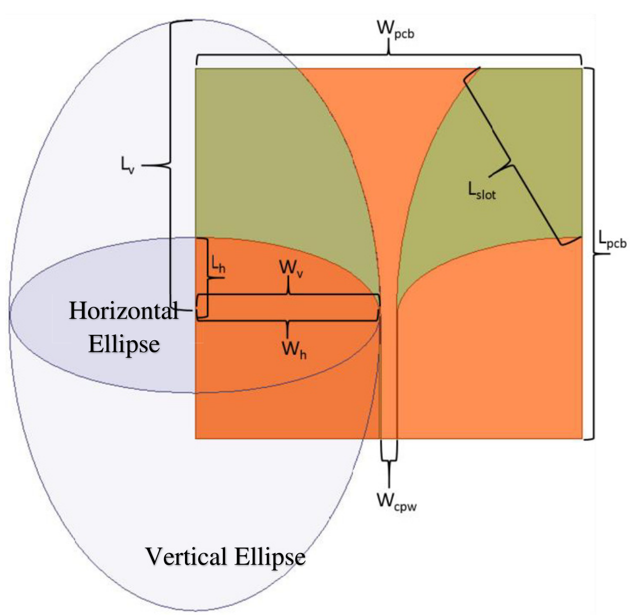

Figure 2. Annotated HFSS design of the antenna.

major axes of vertical and horizontal ellipses which resulted into good impedance match of the antenna in the desirable frequency range. In principle, two slots radiate in their respective directions, and by exploiting the mutual coupling of closely placed slots, an omnidirectional radiation pattern is achieved. Final dimensions of the antenna are given in Table 1.

Table 1. Optimized dimenions of the proposed antenna.

Design parameter	**Optimized Value (mm)**
$\mathbf{L_v}$ (Major axis of vertical ellipse)	75.8
$\mathbf{W_v}$ (Minor axis of vertical ellipse)	48
$\mathbf{L_h}$ (Minor axis of horizontal ellipse)	20
$\mathbf{W_h}$ (Major axis of horizontal ellipse)	47.75
$\mathbf{W_{cpw}}$ (width of CPW feed)	4
$\mathbf{S_{cpw}}$ (separation in the CPW feed)	0.25
$\mathbf{L_{slot}}$ (Length of radiating slot)	45
$\mathbf{L_{pcb}}$ (Length of PCB)	95
$\mathbf{W_{pcb}}$ (Width of PCB)	100

With the dimensions mentioned above in Table 1, the antenna showed decent impedance matching with omnidirectional radiation but it also showed significant back-lobe radiations as well. In order to reduce the back-lobe radiation, two flares of the CPW ground were tapered as shown in Figure 3.

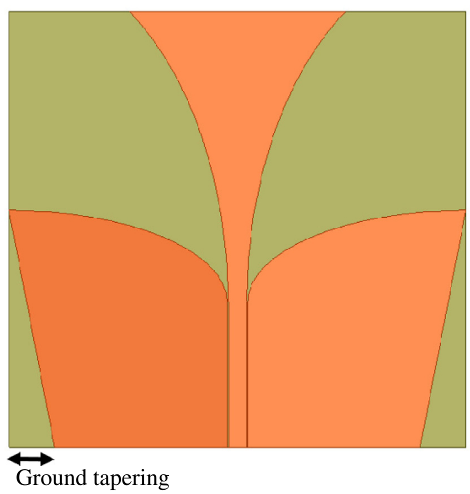

Figure 3. Final antenna design with tapered CPW ground to minimize back lobe radiation.

Figure 4 shows the simulated surface current distribution on the antenna. As can be seen from the figure that the incident surface currents get cancelled by the return currents in the middle of the antenna giving us a null in the boresight (unlike typical vivaldi antennas which give maximum radiation in the boresight). This forms a boundary condition in the middle of the antenna. On either side of this boundary, the surface currents are mutually directed at 120 degrees with the help of two tapered slots. The E fields, which become loosely bound by the gradual increase in slot size, get radiated eventually from the slot ends.

3. ANTENNA FABRICATION

The antenna was fabricated using an LPKF PCB manufacturing machine. The finest feature in the antenna was 250 µm separation gap required to achieve 50 Ω impedance of CPW feedline with a width

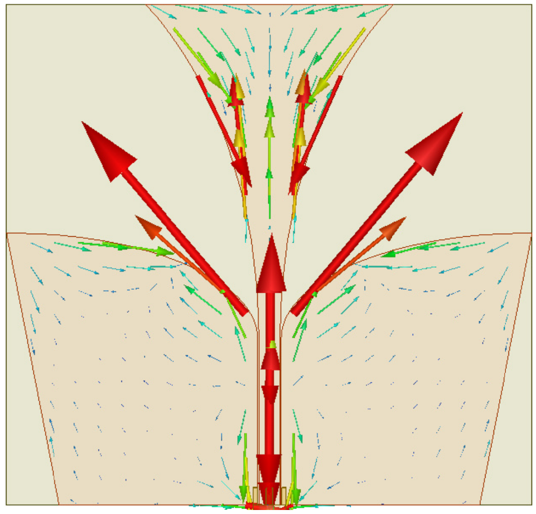

Figure 4. Simulated surface currents on the antenna.

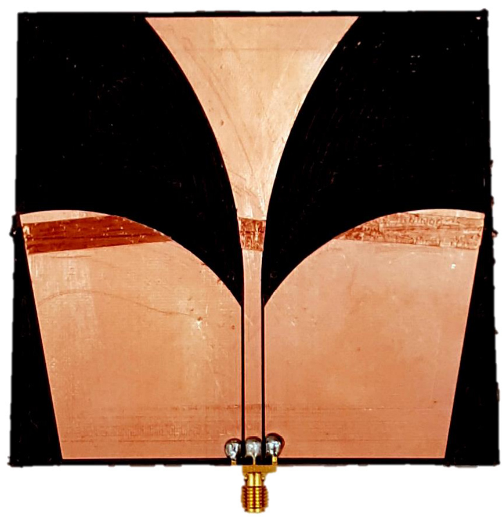

Figure 5. Manufactured antenna based upon a single layer.

of 4 mm. The finest micro-cutter available with the LPKF machine had a resolution of 300 μm, so one can expect a slight variation in the gap of the CPW line which may affect the measured impedance performance of the antenna. The measured results will be discussed in detail in the next section. The final prototype of the antenna is shown in Figure 5.

The antenna was first characterized for its return loss using vector network analyzer and then characterized in a Satimo anechoic chamber to measure its radiation performance. The anechoic chamber was first calibrated using a standard horn antenna and was then used to test the antenna under test (AUT) as shown in Figure 6.

4. RESULTS

4.1. Impedance Matching

The antenna (Figure 2) was designed in HFSS to be used in different frequency bands in UWB range, i.e., starting from 3.1 GHz. Owing to the high impedance offered by elliptically tapered slot, it was quite

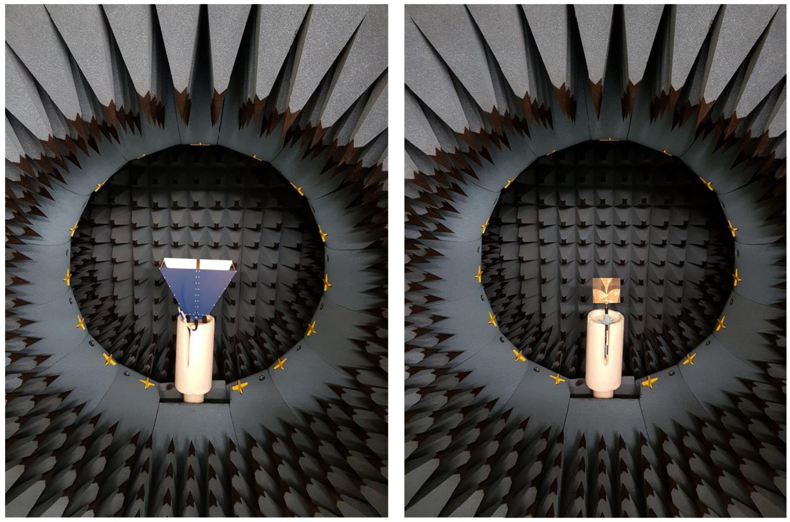

(a) (b)

Figure 6. Antenna characterization in anechoic chamber: (a) calibration using horn antenna. (b) Antenna under test.

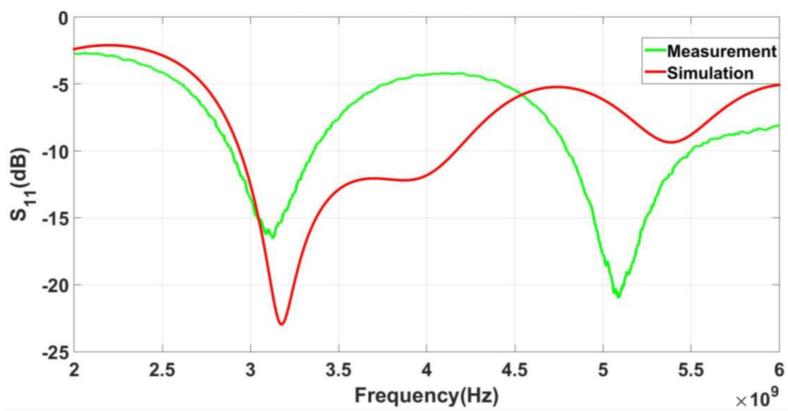

Figure 7. Comparison of simulated and measured return losses of the designed antenna.

challenging to match the antenna to 50 Ω. Prime focus of optimization of the antenna was to maintain good omnidirectional radiation with decent matching in the frequency spectrum of UWB.

After fabrication, the return loss of the antenna was measured using FieldFox Handheld Network Analyser N9923A from Keysight. The comparison of simulations with measurements is shown in Figure 7.

As can be seen from Figure 7, the simulated antenna shows satisfactory matching in two bands of UWB spectrum, i.e., 2.9 GHz–4.2 GHz and the other resonance appears near 5.4 GHz, but this is not a perfect match. In order to investigate this issue, SMA connector has been included in HFSS simulations as can be seen from Figure 8.

As can be seen from Figure 8, the connector's ground plane is in close proximity of the signal conductor, and one can expect variation in its impedance due to the connector. Figure 9 compares the measurements of the antenna with HFSS simulations taking SMA connector into account.

We can clearly see by comparing Figure 7 and Figure 9 that measurements match quite well with the simulations when SMA connector effect is taken into account. The measured return loss shows good matching (VSWR < 2) in the bands of 2.8 GHz–3.4 GHz and 4.8 GHz–5.5 GHz. These frequency bands cover multiple wireless applications such as wireless USB and high throughput Wi-Fi using IEEE

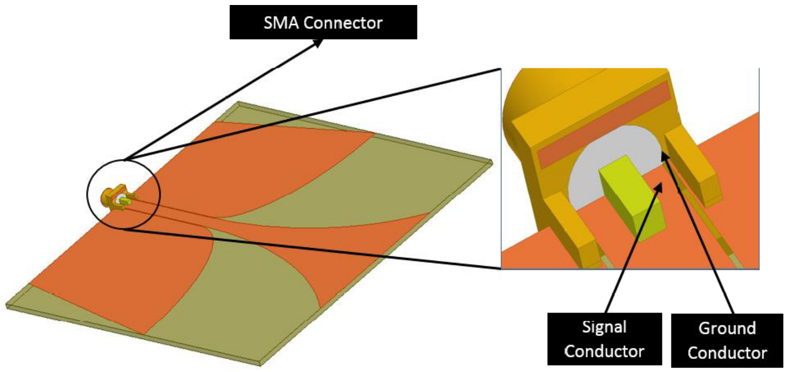

Figure 8. Post-fabrication HFSS simulations along with SMA connector.

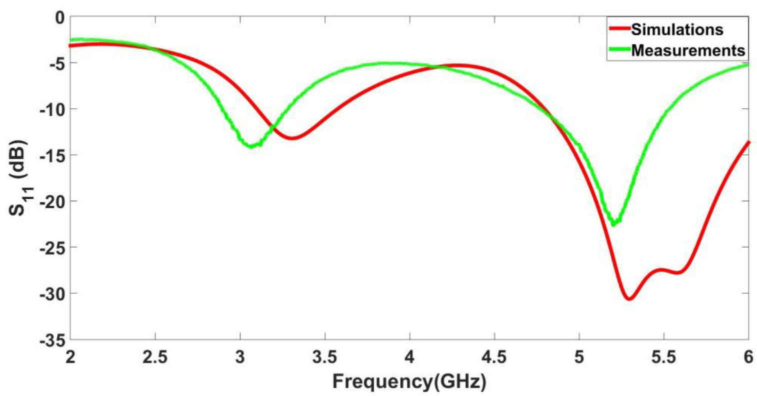

Figure 9. Comparison of simulated (with SMA connector) and measured return losses of the designed antenna.

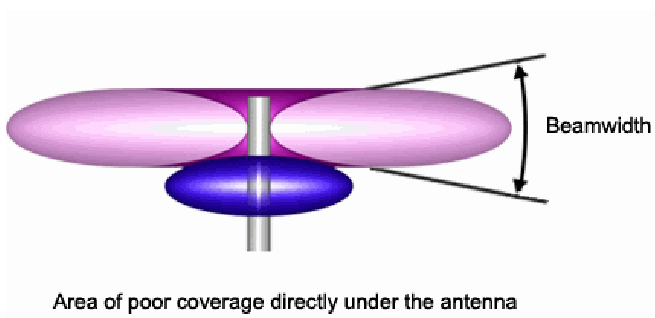

Figure 10. Typical omni-directional radiation pattern with poor coverage [12].

802.11ac wireless networking standard [9, 10]. Multiple techniques such as comb slots [11] are used to extend the impedance matching of conventional end-fire Vivaldi antenna, but those techniques are avoided here in order not to disturb the omnidirectional radiation pattern.

4.2. Radiation Pattern

The reason for compromising the impedance matching is to achieve nice omnidirectional radiation pattern with desirable down-tilt.

As can be seen from Figure 10, a considerable amount of radiated power is lost in the top hemisphere of those omnidirectional antennas which are mounted on roof tops or communication tower heads. In

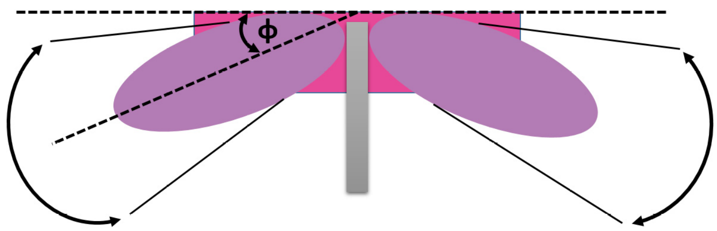

Figure 11. Better coverage achievable through down-tilt (φ).

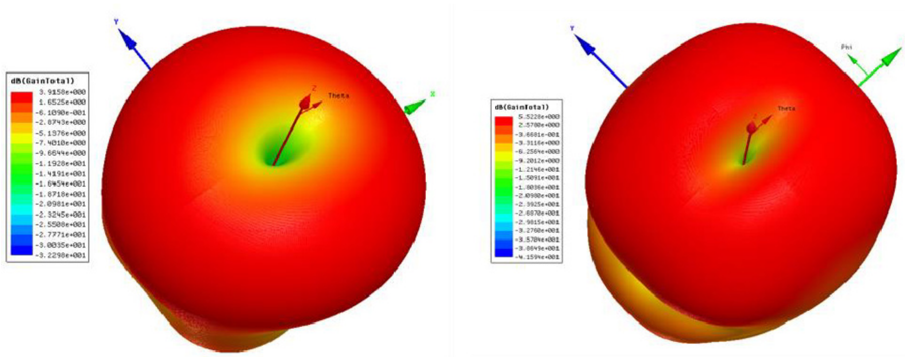

(a) (b)

Figure 12. Measured peak gains at different frequencies in UWB spectrum.

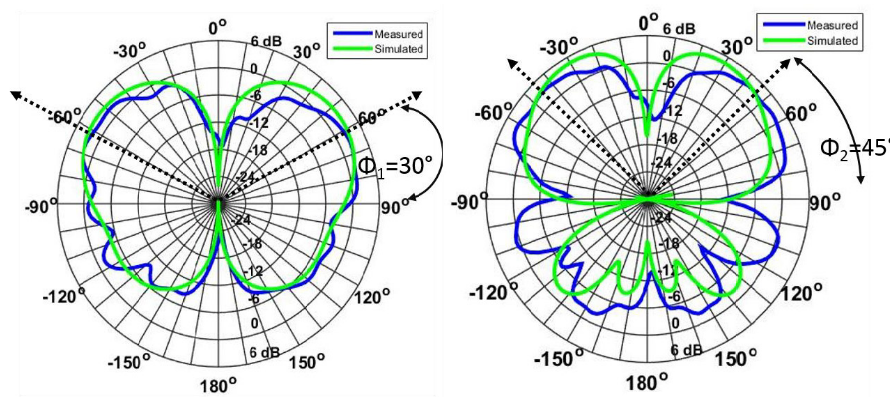

(a) (b)

Figure 13. 2D radiation pattern corresponding to Phi = 90° (YZ axis in Figure 12) cut. (a) At 2.9 GHz. (b) At 5 GHz.

those installations, it is desirable to down-tilt the omnidirectional beam to achieve better coverage as shown in Figure 11.

As the radiating slots in the proposed antenna (Figure 3) have a mutual angle around 120°, we can achieve the desirable down-tilt in its radiation performance. Figure 12 shows the simulated 3D radiation patterns at 3.1 GHz and 5 GHz frequencies.

Simulations and measurements show that we can achieve 30° and 45° of down-tilt in lower (2.8 GHz-3.4 GHz) and higher (4.8 GHz–5.5 GHz) frequency bands, respectively. Figure 13 shows the radiation plots in both the bands.

The maxima of conventional omnidirectional antenna lies at 90° which results into equal radiation coverage of both the hemispheres. It is evident from Figure 13 that the proposed antenna radiates

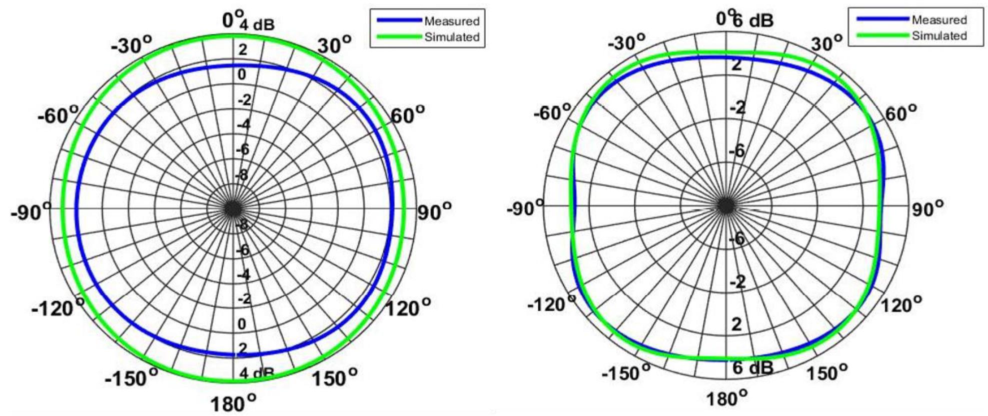

(a) (b)

Figure 14. 2D radiation pattern corresponding to (a) Theta 60° @ 2.9 GHz. (b) Theta 45° @ 5 GHz.

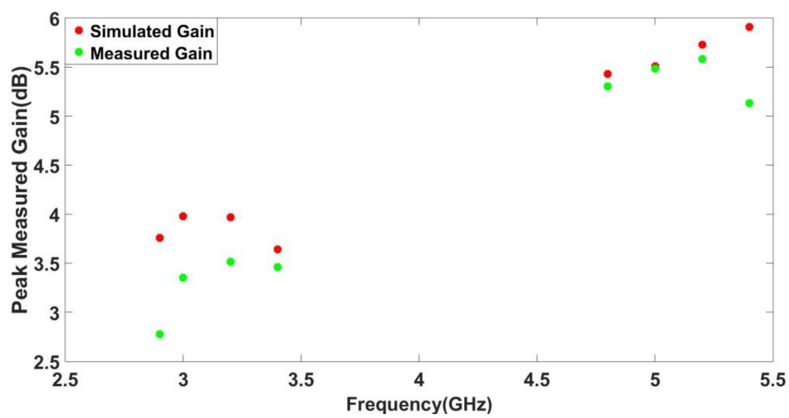

Figure 15. Measured peak gains at different frequencies in UWB spectrum.

maximum at theta (angle with z-axis) 60° and 45° which correspond to down-tilt (difference from 90°) of 30° and 45° at 2.9 GHz and 5 GHz, respectively. It results in better coverage of one of the hemispheres and making the proposed design more suitable for roof-top or tower-top applications. It can also be seen that owing to the ground tapering (Figure 3) antenna radiates minimally (below -6 dB) in the other hemisphere.

Moreover, very smooth omnidirectional radiation with a gain variation of < 1 dB is achieved in both the low and high frequency bands as can be seen from Figure 14.

As evident from Figure 14, the measured gain of more than 2 dB is achieved in the low frequency and 4 dB in the high frequency band. Good correlation exists between simulation and measurements with slightly less gain in measurements, which is expected because the simulations make use of perfect electric conductor (PEC) and do not take conductor losses into account.

Figure 15 shows the comparison of peak simulated as well as measured gains at multiple frequencies of UWB spectrum. The plot shows that the gain and bandwidth achieved is much higher than that achievable with conventional omnidirectional antennas. Moreover, there is a good correspondence between the simulated and measured gains. The simulated gain is slightly higher than the measured one because conductors have been assumed as perfect electric conductor (PEC) in HFSS simulations, so the conductor losses are not included in the simulated gains.

5. CONCLUSION

The paper presents, first of its kind, a dual tapered slot antenna inspired by a Vivaldi structure. The presented antenna makes use of only single layer of PCB and shows 42% measured fractional impedance and radiation bandwidth in two bands of UWB spectrum, i.e., 2.8 GHz–3.4 GHz and 4.8 GHz–5.4 GHz. VSWR is less than 2 dB in these bands, and the measured omnidirectional gain around 5.3 dB (±0.2 dB) in the band of 4.8 GHz–5.4 GHz and 3.2 dB (±0.3 dB) in the band of 2.8 GHz–3.4 GHz is achieved. The proposed antenna shows higher omnidirectional gains because the radiation is concentrated in one of the hemispheres by introducing desirable down-tilt in its radiation pattern. It is successfully shown that the antenna offers desirable down-tilt (30° for lower frequency band and 45° for higher frequency band) for better signal coverage in the hemisphere making it a useful design especially for roof-top applications.

REFERENCES

1. Chen, B., Y.-C. Jiao, F.-C. Ren, and L. Zhang, "Broadband monopole antenna with wide-bandcircular polarization," *Progress In Electromagnetics Research Letters*, Vol. 32, 19–28, 2012.
2. Zhang, W.-X., "Modified tapered slot-line antennas for special applications," *REV Journal on Electronics and Communications*, Vol. 2, No. 3–4, 106–112, 2012.
3. Zhang, P., W.-X. Zhang, and S. J. Tang, "Improved tapered slot-line antennas loaded by grating," *Journal of Electromagnetic Waves and Applications*, Vol. 23, No. 8–9, 1039–1048, 2009.
4. Yngvesson, K. S., T. L. Korzeniowski, Y.-S. Kim, E. L. Kollberg, and J. F. Johansson, "The tapered slot antenna — A new integrated element for millimeter-wave applications," *IEEE Transactions on Microwave Theory and Techniques*, Vol. 37, No. 2, 365–374, 1989.
5. Pandey, G. K., H. Verma, and M. K. Meshram, "Compact antipodal vivaldi antenna for UWB applications," *Electronics Letters*, Vol. 51, No. 4, 308–310, 2015.
6. Yang, Y., Y. Wang, and A. E. Fathy, 'Designof compact vivaldi antenna arrays for UWB see through wall applications," *Progress In Electromagnetics Research*, Vol. 82, 401–418, 2008.
7. Benjamin, A. S. and S. Cook, "Inkjet printing of novel wideband and high gain antennas on low-cost paper substrate," *IEEE Transactions on Antennas and Propagation*, Vol. 60, No. 9, 4148–415, 2012.
8. Fei, P., Y.-C. Jiao, Y. Ding, and F.-S. Zhang, "A compact coplanar waveguide fed wide tapered slot ultra-wideband antenna," *Progress In Electromagnetics Research Letters*, Vol. 25, 77–85, 2011.
9. USB, E., "Wireless USB FAQ," 2016. [Online]. Available: http://www.everythingusb.com/wireless-usb.html#1.
10. Varma, V. K., "Wireless Fidelity — WiFi," Originally published on the IEEE Emerging Technology portal, 2006–2012. [Online]. Available: https://www.ieee.org/about/technologies/emerging/wifi.pdf.
11. Zarrabi, F. B., N. P. Gandji, R. Ahmadian, H. Kuhestani, and Z. Mansouri, "Modification of vivaldi antenna for 2–18 GHz UWB application with substrate integration waveguide structure and comb slots," *ACES Journal*, Vol. 30, No. 8, 844–849, 2015.
12. CISCO, "Omni antenna vs. directional antenna," 2007. [Online]. Available: http://www.cisco.com/c/en/us/support/docs/wireless-mobility/wireless-lan-wlan/82068-omni-vs-direct.html.